

# NLO QCD corrections to Higgs boson production plus three jets in gluon fusion

G. Cullen,<sup>1</sup> H. van Deurzen,<sup>2</sup> N. Greiner,<sup>2</sup> G. Luisoni,<sup>2</sup> P. Mastrolia,<sup>2,3</sup>  
 E. Mirabella,<sup>2</sup> G. Ossola,<sup>4,5</sup> T. Peraro,<sup>2</sup> and F. Tramontano<sup>6,7</sup>

<sup>1</sup>*Deutsches Elektronen-Synchrotron DESY, Platanenallee 6, 15738 Zeuthen, Germany*

<sup>2</sup>*Max-Planck-Institut für Physik, Föhringer Ring 6, 80805 München, Germany*

<sup>3</sup>*Dipartimento di Fisica e Astronomia, Università di Padova,*

*and INFN Sezione di Padova, via Marzolo 8, 35131 Padova, Italy*

<sup>4</sup>*New York City College of Technology, City University of New York, 300 Jay Street, Brooklyn NY 11201, USA*

<sup>5</sup>*The Graduate School and University Center, City University of New York, 365 Fifth Avenue, New York, NY 10016, USA*

<sup>6</sup>*Dipartimento di Fisica, Università degli studi di Napoli “Federico II”, I-80125 Napoli, Italy*

<sup>7</sup>*INFN, Sezione di Napoli, I-80125 Napoli, Italy*

We report on the calculation of the cross section for Higgs boson production in association with three jets via gluon fusion, at next-to-leading-order (NLO) accuracy in QCD, in the infinite top-mass approximation. After including the complete NLO QCD corrections, we observe a strong reduction in the scale dependence of the result, and an increased steepness in the transverse momentum distributions of both the Higgs and the leading jets. The results are obtained with the combined use of GOSAM, SHERPA, and the MADDIPOLE/MADEVENT framework.

## INTRODUCTION

The latest results reported by the ATLAS and CMS collaborations have confirmed with a higher confidence-level the existence of a new neutral boson with mass of about 125 – 126 GeV and spin different from one [1, 2], and suggest that the new particle has indeed the features of a Higgs boson, thus confirming the validity of the electroweak symmetry breaking mechanism. Although the evidence accumulated so far is compatible with the hypothesis that the new resonance is the Higgs particle predicted by the Standard Model (SM) with the  $J^P = 0^+$  [3, 4], in order to confirm its nature, further high-precision studies on spin, parity, coupling strengths and branching ratios are mandatory.

In  $pp$ -collisions, the dominant Higgs production mechanism proceeds via gluon fusion (GF),  $gg \rightarrow H$ , where the coupling of the Higgs to the gluons is mediated by a heavy quark loop.

Another important production channel for the Higgs boson is Vector Boson Fusion (VBF), since it allows a direct measurement of the coupling of the Higgs to the massive electroweak bosons [5]. The cross section in the VBF channel is about an order of magnitude smaller than in GF, and even after applying specific cuts, the latter remains the main source of background for Higgs production in VBF.

For these reasons, the calculation of higher order corrections for the GF production of a Higgs boson in association with jets has received a lot of attention in the theory community over the past decades [6–8].

The leading order (LO) contribution to the production of a Higgs boson in association with two jets ( $Hjj$ ), and three jets ( $Hjjj$ ) have been computed respectively in Refs. [9, 10], and in the recent Ref. [11]. These calculations have been performed retaining the full top-mass ( $m_t$ ) dependence, and showed the validity of the large



Figure 1. Sample hexagon diagrams which enter in the six-parton one-loop amplitudes for  $q\bar{q} \rightarrow Hq\bar{q}g$  and  $gg \rightarrow Hggg$ . The dot represents the effective  $ggH$  vertex.

top-mass approximation ( $m_t \rightarrow \infty$ ) whenever the mass of the Higgs particle and the  $p_T$  of the jets are not sensibly larger than the mass of the top quark. In this approximation, the Higgs coupling to two gluons, which at LO is mediated by a top-quark loop, becomes independent of  $m_t$ , and it can be described by an effective operator [12], as

$$\mathcal{L}_{\text{eff}} = -\frac{g_{\text{eff}}}{4} H \text{tr} (G_{\mu\nu} G^{\mu\nu}) . \quad (1)$$

In the  $\overline{\text{MS}}$  scheme, the coefficient  $g_{\text{eff}}$  reads [13, 14]

$$g_{\text{eff}} = -\frac{\alpha_s}{3\pi v} \left( 1 + \frac{11}{4\pi} \alpha_s \right) + \mathcal{O}(\alpha_s^3) , \quad (2)$$

in terms of the Higgs vacuum expectation value  $v$ , set to  $v = 246$  GeV. The operator (1) leads to new Feynman rules, with vertices involving the Higgs field and up to four gluons.

The leading order contributions to  $Hjjj$ , both for VBF and GF (in the  $m_t \rightarrow \infty$  limit), have been calculated in [15]. However, while the VBF calculation is available also at NLO [16], the computation of the Higgs plus three jets in GF is still missing.

Elaborating on the techniques employed in the recent calculation of the NLO contributions to  $Hjj$  production at the LHC [17], in this letter we report on the calculation of the cross section for  $pp \rightarrow Hjjj$  in GF at NLO accuracy in QCD, within the infinite  $m_t$  approximation.

This calculation is challenging due to the complexity of both the real-emission contributions and of the virtual corrections, which involve more than 10,000 one-loop Feynman diagrams with up to rank-seven hexagons.

## COMPUTATIONAL SETUP

A complete next-to-leading order calculation requires the evaluation of virtual and real emission contributions.

For the computation of the virtual corrections we use a code generated by the program package GOSAM [18], which combines automated diagram generation and algebraic manipulation [19–22] with integrand-level reduction techniques [23–29].

In order to deal with the complexity level of the considered calculation, the GOSAM code has been enhanced. On the one side, the generation algorithm has been improved by a more efficient diagrammatic layout: Feynman diagrams are grouped according to their topologies, namely global numerators are constructed by combining diagrams that have a common set, or subset, of denominators, irrespectively of the specific particle content. On the other side, additional improvements in the performances of GOSAM have been achieved by exploiting the optimized manipulation of polynomial expressions available in FORM 4.0 [30]. The new developments of GOSAM, regarding the improved generation and reduction algorithms, will be properly discussed in a dedicated communication.

Within the GOSAM framework the virtual corrections are evaluated using the  $d$ -dimensional integrand-level decomposition implemented in the SAMURAI library [31, 32], which allows for the combined determination of both cut-constructible and rational terms at once. Alternatively, a tensorial decomposition [33, 34] via GOLEM95 is used as a rescue system. After the reduction, all relevant master integrals are computed by means of QCDLOOP [35, 36], ONELOOP [37], or GOLEM95C [38].

The basic partonic processes contributing to  $Hjjj$  production are listed in Tab. I, together with the corresponding number of Feynman diagrams and the approximate computing time per phase-space point after summing over color and helicities. Representative one-loop diagrams are depicted in Figure 1.

SUBPROCESS	DIAGRAMS	TIME/PS-POINT [sec]
$q\bar{q} \rightarrow Hq'\bar{q}'g$	467	0.29
$q\bar{q} \rightarrow Hq\bar{q}g$	868	0.60
$gg \rightarrow Hq\bar{q}g$	2519	3.9
$gg \rightarrow Hggg$	9325	20

Table I. Number of Feynman diagrams and computing time per phase-space point for each subprocess, on a Intel i7 960 (3.20GHz) CPU. The code is compiled with the Intel fortran compiler `ifort` (with optimization `O2`).

The ultraviolet (UV), the infrared (IR), and the collinear singularities are regularized using dimensional reduction (DRED). UV divergences have been renormalized in the  $\overline{\text{MS}}$  scheme. In the case of LO [NLO] contributions we describe the running of the strong coupling constant with one-loop [two-loop] accuracy.

The effective  $Hgg$  coupling leads to integrands that may exhibit numerators with rank larger than the number of the denominators. In general, for these cases, the parametrization of the residues at the multiple-cut has to be extended and, as a consequence, the decomposition of any one-loop amplitude acquires new master integrals (MIs) [28]. The extended integrand decomposition has been implemented in the SAMURAI library.

Remarkably, for the processes at hand, it has been proven that the higher-rank terms are proportional to the loop momentum squared, which simplifies against a denominator, hence generating lower-point integrands where the rank is again equal to the number of denominators [17]. Consequently, the coefficients of the new MIs have to vanish identically, as explicitly verified. The available options in GOSAM for the algebraic manipulation of the integrands allow for the automatic computation of the virtual corrections in two different ways. In the first approach, GOSAM decomposes the four-dimensional part of the numerators using the extended-rank decomposition, and adds the analytic results of the rational terms (generated from the extra-dimensional part). In the second approach, the regular decomposition of SAMURAI, without the higher rank extension, is employed on the whole  $d$ -dimensional integrands. We checked that both approaches provide identical answers. In the following, we adopt the second strategy, which proved to be numerically more efficient.

The double and the single poles conform to the universal singular behavior of dimensionally regulated one-loop amplitudes [39]. We also checked that our results fulfill gauge invariance: when substituting the polarization vectors of one or more gluons with the corresponding momenta, the result for the amplitudes, after summing over all diagrams, are indeed vanishing. Additional information about the virtual contributions can be found in the Appendix.

Results for the cross section are obtained with a hybrid setup which combines the features of two different Monte Carlo (MC) tools. For the generation and integration of the Born and of the virtual contributions, we used an automated framework for fixed order NLO QCD calculations, based on the interplay of GOSAM and SHERPA [40], where the tree-level matrix elements are obtained with the AMEGIC [41] library. The integration is carried out by generating  $\mathcal{O}(10^6)$  events, sampled on a MC grid trained on the Born matrix element, and weighted with the sum of the Born and the virtual amplitudes.

For the integration of the real-radiation terms, the dipole-subtraction terms, and the integrated dipoles, we

employ a combination of MADGRAPH [42, 43] (matrix elements), MADDIPOLE [44, 45] (subtraction terms), and MADEVENT [46] (numerical integration). We verified the independence of our result under the variation of the so called  $\alpha$ -parameter that fixes the amount of subtractions around the divergences of the real corrections.

We first proved the consistency of our hybrid MC integration on  $pp \rightarrow Hjj$ , verifying that the full cross section at NLO agrees with the corresponding result for the integration of both the virtual and the real corrections obtained by the interplay of SHERPA and GOSAM alone. Moreover, for the process under consideration, namely  $pp \rightarrow Hjjj$ , we found excellent agreement between MADGRAPH and SHERPA for the LO cross section.

### INTEGRATED CROSS SECTION

In the following, we present results for the integrated cross section of Higgs boson plus three jets production at the LHC, for a center-of-mass energy of 8 TeV. The mass of the Higgs boson is set to  $m_H = 125$  GeV.

Jets are clustered using the `antikt`-algorithm implemented in FASTJET [47–49] with radius  $R = 0.5$  and a minimum transverse momentum of  $p_{T,jet} > 20$  GeV and pseudorapidity  $|\eta| < 4.0$ . The LO cross section is computed with the LO parton-distribution functions `cteq6L1`, whereas at NLO we use `cteq6mE` [50].

Everywhere, but in the effective coupling of the Higgs to the gluons, the renormalization and factorization scales are set to

$$\mu_F = \mu_R = \frac{\hat{H}_T}{2} = \frac{1}{2} \left( \sqrt{m_H^2 + p_{T,H}^2} + \sum_i |p_{T,i}| \right), \quad (3)$$

where the sum runs over the final state jets. The strong coupling is therefore evaluated at different scales according to  $\alpha_s^5 \rightarrow \alpha_s^2(m_H)\alpha_s^3(\hat{H}_T/2)$ . The theoretical uncertainties are estimated by varying the scales by factors of 0.5 and 2.0 respectively. In the effective coupling the scale is kept at  $m_H$ . Within this setup we obtain the following total cross section at LO and NLO:

$$\sigma_{\text{LO}}[\text{pb}] = 0.962_{-0.31}^{+0.51}, \quad \sigma_{\text{NLO}}[\text{pb}] = 1.18_{-0.22}^{+0.01}.$$

The scale dependence of the total cross section, depicted in Fig. 2, is strongly reduced by the inclusion of the NLO contributions.

In Figs. 3 and 4, we show the  $p_T$  distributions of the three jets and of the Higgs boson, respectively. The NLO corrections enhance all distributions for  $p_T$  values lower than 150 – 200 GeV, whereas their contribution is negative at higher  $p_T$ . This behavior is explicitly shown in the lower part of Fig. 4 for the case of the Higgs boson.

This study also shows that the virtual contributions for  $pp \rightarrow Hjjj$  generated by GOSAM can be successfully

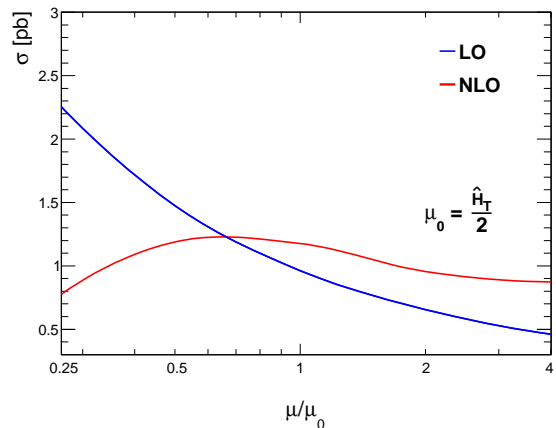


Figure 2. Scale dependence of the total cross section at LO and NLO.

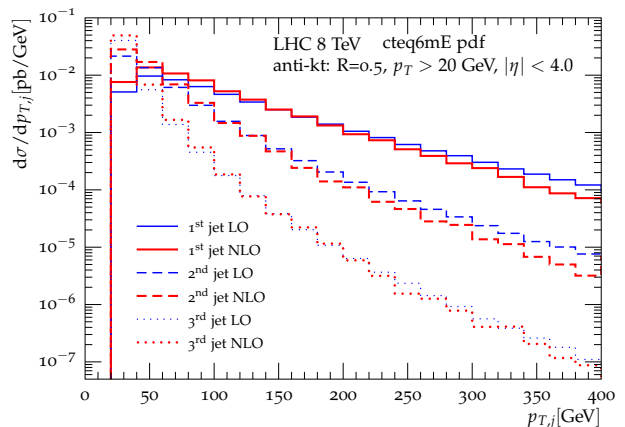


Figure 3. Transverse momentum ( $p_T$ ) distributions for the first, second, and third leading jet.

paired with available Monte Carlo programs to aim at further phenomenological analyses.

We thank Thomas Hahn and Gudrun Heinrich for discussions and comments on the manuscript, and Marek Schönherr for assistance with the usage of SHERPA. The work of G.C. was supported by DFG SFB-TR-9 and the EU TMR Network LHCPHENonet. The work of H.v.D., G.L., P.M., and T.P. was supported by the Alexander von Humboldt Foundation, in the framework of the Sofja Kovaleskaja Award 2010, endowed by the German Federal Ministry of Education and Research. G.O. was supported in part by the National Science Foundation under Grant PHY-1068550. F.T. acknowledges partial support by MIUR under project 2010YJ2NYW. G.C. and G.O. wish to acknowledge the kind hospitality of the Max-Planck-Institut für Physik in Munich at several stages during the completion of this project. This research used computing resources from the Rechenzentrum Garching

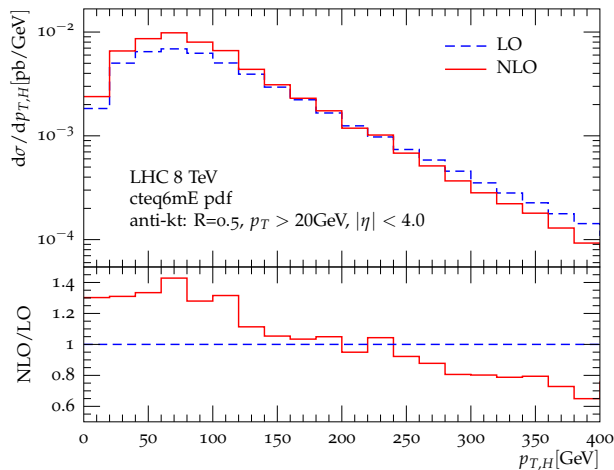


Figure 4. Transverse momentum ( $p_T$ ) distributions for the Higgs boson.

and the New York City College of Technology.

#### APPENDIX: SELECTED RESULTS FOR THE VIRTUAL CONTRIBUTIONS

The numerical values of the one-loop sub-amplitudes, defined as

$$\frac{2 \Re \{ \mathcal{M}^{\text{tree-level}} \mathcal{M}^{\text{one-loop}} \}}{(\alpha_s/2\pi) |\mathcal{M}^{\text{tree-level}}|^2} \equiv \frac{a_{-2}}{\epsilon^2} + \frac{a_{-1}}{\epsilon} + a_0, \quad (4)$$

and evaluated at the non-exceptional phase space point given in Tab. II, are collected in Tab. III. The values of the double and the single poles conform to the universal singular behavior of dimensionally regulated one-loop amplitudes [39]. The precision of the finite parts is estimated by re-evaluating the amplitudes for a set of momenta rotated by an arbitrary angle about the axis of collision.

In Fig. 5, we present the results for the finite part  $a_0$  of the virtual matrix elements for the various subprocesses calculated along a certain one-dimensional curve in the space of final state momenta. Starting from the phase space point in Tab. II, in which the initial partons lie along the  $z$ -axis, we generate new configurations by rotating the final state momenta by an angle  $\theta \in [0, 2\pi]$  about the  $y$ -axis.

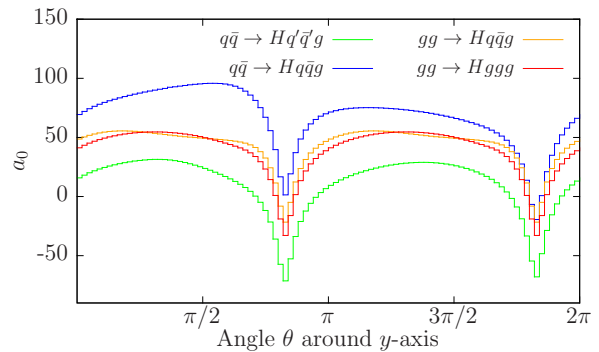


Figure 5. Finite-term  $a_0$  of the virtual matrix-elements for  $q\bar{q} \rightarrow Hq'\bar{q}'g$  (green),  $q\bar{q} \rightarrow Hq\bar{q}g$  (blue),  $gg \rightarrow Hq\bar{q}g$  (orange),  $gg \rightarrow Hggg$  (red).

[1] G. Aad et al. (ATLAS Collaboration), Phys.Lett. **B716**, 1 (2012), 1207.7214.  
[2] S. Chatrchyan et al. (CMS Collaboration), Phys.Lett. **B716**, 30 (2012), 1207.7235.  
[3] ATLAS-CONF-2013-040 (2013).  
[4] CMS-PAS-HIG-13-005 (2013).

[5] D. Zeppenfeld, R. Kinnunen, A. Nikitenko, and E. Richter-Was, Phys.Rev. **D62**, 013009 (2000), hep-ph/0002036.  
[6] S. Dittmaier et al. (LHC Higgs Cross Section Working Group) (2011), 1101.0593.  
[7] S. Dittmaier, S. Dittmaier, C. Mariotti, G. Passarino, R. Tanaka, et al. (2012), 1201.3084.  
[8] S. Heinemeyer et al. (The LHC Higgs Cross Section Working Group) (2013), 1307.1347.  
[9] V. Del Duca, W. Kilgore, C. Oleari, C. Schmidt, and D. Zeppenfeld, Phys.Rev.Lett. **87**, 122001 (2001), hep-ph/0105129.  
[10] V. Del Duca, W. Kilgore, C. Oleari, C. Schmidt, and D. Zeppenfeld, Nucl.Phys. **B616**, 367 (2001), hep-ph/0108030.  
[11] F. Campanario and M. Kubocz (2013), 1306.1830.  
[12] F. Wilczek, Phys.Rev.Lett. **39**, 1304 (1977).  
[13] A. Djouadi, M. Spira, and P. Zerwas, Phys.Lett. **B264**, 440 (1991).  
[14] S. Dawson, Nucl.Phys. **B359**, 283 (1991).  
[15] V. Del Duca, A. Frizzo, and F. Maltoni, JHEP **0405**, 064 (2004), hep-ph/0404013.  
[16] T. Figy, V. Hankele, and D. Zeppenfeld, JHEP **0802**, 076 (2008), 0710.5621.  
[17] H. van Deurzen, N. Greiner, G. Luisoni, P. Mastrolia, E. Mirabella, et al., Phys.Lett. **B721**, 74 (2013), 1301.0493.  
[18] G. Cullen, N. Greiner, G. Heinrich, G. Luisoni, P. Mastrolia, et al., Eur.Phys.J. **C72**, 1889 (2012), 1111.2034.  
[19] P. Nogueira, J.Comput.Phys. **105**, 279 (1993).  
[20] J. A. M. Vermaseren (2000), math-ph/0010025.  
[21] T. Reiter, Comput.Phys.Commun. **181**, 1301 (2010), 0907.3714.  
[22] G. Cullen, M. Koch-Janusz, and T. Reiter, Comput.Phys.Commun. **182**, 2368 (2011), 1008.0803.  
[23] G. Ossola, C. G. Papadopoulos, and R. Pittau, Nucl.Phys. **B763**, 147 (2007), hep-ph/0609007.  
[24] G. Ossola, C. G. Papadopoulos, and R. Pittau, JHEP **0707**, 085 (2007), 0704.1271.  
[25] R. K. Ellis, W. T. Giele, and Z. Kunszt, JHEP **03**, 003 (2008), 0708.2398.  
[26] G. Ossola, C. G. Papadopoulos, and R. Pittau, JHEP **0805**, 004 (2008), 0802.1876.

PARTICLE	$E$	$p_x$	$p_y$	$p_z$
$p_1$	250.00000000000000	0.0000000000000000	0.0000000000000000	250.00000000000000
$p_2$	250.00000000000000	0.0000000000000000	0.0000000000000000	-250.00000000000000
$p_3$	131.06896655823209	27.707264814722667	-13.235482900394146	24.722529472591685
$p_4$	164.74420140597425	-129.37584098675183	-79.219260486951597	-64.240582451932028
$p_5$	117.02953632773803	54.480516624273569	97.990504664150677	-33.550658370629378
$p_6$	87.157295708055642	47.188059547755266	-5.5357612768047906	73.068711349969661

Table II. Benchmark phase space point for Higgs plus three jets production. Particles are ordered as in Tab. I.

	$gg \rightarrow Hggg$	$gg \rightarrow Hq\bar{q}g$	$q\bar{q} \rightarrow Hq\bar{q}g$	$q\bar{q} \rightarrow Hq'\bar{q}'g$
$a_0$	<u>41.22878766741685</u>	<u>48.68424134989478</u>	<u>69.32351140474695</u>	<u>15.79262767177915</u>
$a_{-1}$	<u>-47.16715419132659</u>	<u>-36.08277728077228</u>	<u>-29.98862932963659</u>	<u>-32.35320587073968</u>
$a_{-2}$	<u>-14.99999999999991</u>	<u>-11.66666666666683</u>	<u>-8.33333333333339</u>	<u>-8.33333333333398</u>

Table III. Numerical results for the four subprocesses listed in Tab. I evaluated at the phase space point of Tab. II. The accuracy of the result is indicated by the underlined digits.

- [27] P. Mastrolia, G. Ossola, C. Papadopoulos, and R. Pittau, JHEP **0806**, 030 (2008), 0803.3964.
- [28] P. Mastrolia, E. Mirabella, and T. Peraro, JHEP **1206**, 095 (2012), 1203.0291.
- [29] P. Mastrolia, E. Mirabella, G. Ossola, and T. Peraro, Phys.Lett. **B718**, 173 (2012), 1205.7087.
- [30] J. Kuipers, T. Ueda, J. Vermaseren, and J. Vollinga, Comput.Phys.Commun. **184**, 1453 (2013), 1203.6543.
- [31] P. Mastrolia, G. Ossola, T. Reiter, and F. Tramontano, JHEP **1008**, 080 (2010), 1006.0710.
- [32] P. Mastrolia, E. Mirabella, G. Ossola, T. Peraro, and H. van Deurzen, PoS **LL2012**, 028 (2012), 1209.5678.
- [33] T. Binoth, J.-P. Guillet, G. Heinrich, E. Pilon, and T. Reiter, Comput.Phys.Commun. **180**, 2317 (2009), 0810.0992.
- [34] G. Heinrich, G. Ossola, T. Reiter, and F. Tramontano, JHEP **1010**, 105 (2010), 1008.2441.
- [35] G. van Oldenborgh, Comput.Phys.Commun. **66**, 1 (1991).
- [36] R. K. Ellis and G. Zanderighi, JHEP **02**, 002 (2008), 0712.1851.
- [37] A. van Hameren, Comput.Phys.Commun. **182**, 2427 (2011), 1007.4716.
- [38] G. Cullen, J. Guillet, G. Heinrich, T. Kleinschmidt, E. Pilon, et al., Comput.Phys.Commun. **182**, 2276 (2011), 1101.5595.
- [39] S. Catani, S. Dittmaier, and Z. Trocsanyi, Phys.Lett. **B500**, 149 (2001), hep-ph/0011222.
- [40] T. Gleisberg, S. Hoeche, F. Krauss, M. Schonherr, S. Schumann, et al., JHEP **0902**, 007 (2009), 0811.4622.
- [41] F. Krauss, R. Kuhn, and G. Soff, JHEP **0202**, 044 (2002), hep-ph/0109036.
- [42] T. Stelzer and W. Long, Comput.Phys.Commun. **81**, 357 (1994), hep-ph/9401258.
- [43] J. Alwall, P. Demin, S. de Visscher, R. Frederix, M. Herquet, et al., JHEP **0709**, 028 (2007), 0706.2334.
- [44] R. Frederix, T. Gehrmann, and N. Greiner, JHEP **0809**, 122 (2008), 0808.2128.
- [45] R. Frederix, T. Gehrmann, and N. Greiner, JHEP **1006**, 086 (2010), 1004.2905.
- [46] F. Maltoni and T. Stelzer, JHEP **0302**, 027 (2003), hep-ph/0208156.
- [47] M. Cacciari and G. P. Salam, Phys.Lett. **B641**, 57 (2006), hep-ph/0512210.
- [48] M. Cacciari, G. P. Salam, and G. Soyez, JHEP **0804**, 063 (2008), 0802.1189.
- [49] M. Cacciari, G. P. Salam, and G. Soyez, Eur.Phys.J. **C72**, 1896 (2012), 1111.6097.
- [50] J. Pumplin, D. Stump, J. Huston, H. Lai, P. M. Nadolsky, et al., JHEP **0207**, 012 (2002), hep-ph/0201195.